ISSN 1392–1320 MATERIALS SCIENCE (MEDŽIAGOTYRA). Vol. 28, No. 2. 2022

Wear Performance of Boronized Layer of Iron-based Powder Metallurgy Materials

Huimin FANG [1, 2] *, Liansen XIA [3], Qingping YU [3], Guangsheng ZHANG [1, 3]

[1] *Institute of Mechanical Engineering, Anhui Technical College of Mechanical and Electrical Engineering, Wuhu, Anhui 241000, China*
[2] *Electromechanical Institute, Nanjing University of Aeronautics and Astronautics, Nanjing, Jiangsu 210016, China*
[3] *School of Materials Science and Engineering, Anhui Polytechnic University, Wuhu, Anhui 241006, China*

crossref http://dx.doi.org/10.5755/j02.ms.28688

Received 23 March 2021; accepted 24 May 2021

Iron-based specimens with boronized layers were prepared by boriding at 800 ℃, 900 ℃ and 1000 ℃ for 3, 5, and 7 hours, respectively. The thickness, microstructure, surface roughness, friction, and wear performance were studied. Results showed that the process parameters such as temperature, the time of boriding have remarkable impact on the thickness of the boronized layer. Dual-phase was generated at 1000 ℃ which lead to increased brittleness, lower surface hardness, and decreased adhesion to the substrate. Compared with specimens boronized at 1000 ℃ and 800 ℃, the surface structure of the boronized layer of specimens boronized at 900 ℃ is denser and uniform, the wear track is not damaged. The average friction coefficient and mass loss by wear of specimens boronized at 900 ℃ are smaller than that of boronized at 1000 ℃ and 800 ℃, indicating that specimens borided at 900 ℃ behave excellent friction and wear performance.
Keywords: boronized layer, adhesion test, friction and wear, mass loss.

1. INTRODUCTION

Due to their considerable economic benefits and excellent physical and mechanical properties, iron-based materials are the largest category of powder metallurgical materials used in the automotive parts manufacturing industry for the preparation of automotive brake disc materials, gears, bearings, etc. Currently, the development of high-strength, high-wear resistance powder metallurgical parts has become the main development direction and research topic in powder metallurgy [1, 2]. However, the aging wear caused by extreme service conditions of mechanical parts will reduce the service life of parts and, in serious cases, can cause serious economic losses [3]. Boronizing can improve the surface properties such as wear resistance, corrosion resistance, and oxidation resistance of engineering components effectively. As a heat treatment method of surface strengthening, boronizing can resist the aging wear to a certain extent to extend the service life [4 – 7]. The most widely used method of boronizing is the solid particle packing boronizing method because of its technical advantages and cost-effectiveness, as well as its advantages of easy control of the thickness and structure of the boronized layer [8, 9]. In the process of high-temperature boronizing, two types of borides such as FeB and Fe_2B are formed according to the Fe-B phase diagram as the B atoms are absorpted and diffused into the lattice of matrix metal. As the concentration of B decreases from the surface to the inside, the FeB phase with boron-rich will generate from the surface, and the Fe_2B phase with iron-rich is generated between the the surface and the base metal [10, 11]. However, single-phase Fe_2B is superior to the dual phase (FeB + Fe_2B) because of the more brittleness and hardness on the FeB than Fe_2B. The structure with a single phase (Fe_2B) is more ideal than that with dual-layer containing FeB and Fe_2B phases in industrial applications. The difference between the coefficients of thermal expansion of the FeB ($\alpha_{FeB} = 23\times10^{-6}$ /℃) and Fe_2B ($\alpha_{Fe_2B}=7.85\times10^{-6}$/℃) phases is large [12], so cracks often form on the FeB/Fe_2B and the formation of a single or dual-phase depends on the process parameters such as temperature, the time of boriding, the chemical composition of the matrix metal and the boriding reagent. Therefore, many scholars researched on this. OA Gómez-Vargas et al. [13] used solid boride AISI 1025 steel and explored its tribological characteristics. The existence of a Fe_2B layer boride on the surface of AISI 1025 steel has nothing to do with the process temperature. The average friction factor is reduced to 0.030 ~ 0.015 through boriding treatment based on 0.107 ~ 0.105 of the substrate materials. Telasang et al. [14] obtained a hardness value of up to 300 HV on the surface of AISI H13 hot-worked tool steels that higher than the hardened and tempered surface, through microdynamics wear tests with different laser powers. In addition, they obtained lower friction coefficient values, which reduced the wear of the laser surface-engineered specimens. Ramdane et al. [15] studied the effect of nitriding and boronizing composite surface treatments on the microstructure, wear and corrosion properties. They concluded that the boronized 4130 steel had the lowest surface friction wear coefficient and the lowest corrosion rate. Compared with that of the boronizing treatment, the carburizing rate of the nitriding and boronizing treatment was lower. Increasing the diffusion time of the boronizing

* Corresponding author: Tel.: 0553-5975091; fax: 0553-5975091.
E-mail address: *0122000353@ahcme.edu.cn* (H. Fang)

treatment from 5 h to 8 h shows that the boronized layer will be thicker and induce the formation of FeB, Fe_2B, CrB, MnB, and MnB_2, resulting in high hardness, low friction factor and low corrosion loss. The existence of nitrogen and carbon influences the boronized layer greatly, which reduces the thickness and hardness of the boronized layer, and the boron surface treatment reduces the depth and hardness of iron boride.

Powder granular materials are widely used in the manufacturing field due to their light weight and good structure. But defects like decompaction and pores inherent in material restrict its strength and tribological properties. Surface strengthening technology such as boriding can notably improve material tribological performance but there are few studies on the wear behavior of the boronized layer of powder granular materials. Iron-based powder granular materials were boronized to improve the wear performance in the experiment, and the influence of process parameters such as temperature, the time of boriding on the thickness of the boronized layer are also discussed.

2. EXPERIMENTAL

2.1. Materials

Iron-based materials with chemical compositions of 2.4 wt.% C, 1.0 wt.% Si, 0.2 wt.% Al, 0.2 wt.% Ni, 0.1 wt.% Mg, 0.1 wt.% Cr, 0.1 wt.% Mn, and 95.9 wt.% Fe were selected as the substrates. Before embedding boronizing treatment, large iron-based specimens were cut into cuboids of 25 mm × 10 mm × 5 mm size by a wire cutting machine. The specimens were polished to relative smoothness by #2000 silicon carbide metallographic sandpaper, rinsed with water, degreased by ultrasonic cleaning in acetone for ten minutes, rinsed with alcohol, and dried with cold air from a hair dryer. The formula of the boronizing agent used is 10 wt.% B_4C + 80 wt.% SiC + 5 wt.% KBF_4 + 5 wt.% C. The boronizing container was a 30 mL ceramic crucible. Then, the boronizing agent was fully embedded to ensure that the specimen was in the centre of the crucible position. Before sealing, a layer of 1300 one-component super high-temperature structural adhesive should be applied on the inner wall of the crucible lid, and after the lid is closed, a layer should also be applied on the outer wall to ensure good sealing performance. The entire chemical heat treatment process was performed in a muffle furnace, the sintering temperatures were set to 800 ℃, 900 ℃, and 1000 ℃, the holding times were 3 h, 5 h, and 7 h, and specimens were cooled by the furnace. After the sintered specimen was removed from the furnace, approximately 2 ~ 3 cm sections were cut from either end of the specimen using a cutting machine, and an inlaying machine with common inlaying powder was used to obtain a cylindrical specimen with the substrate embedded in the centre. The specimen was polished to absolute smoothness by #400, #800, #1200, #1500, and #2000 metallographic silicon carbide abrasive paper and then placed in a diamond abrasive paste polishing machine to achieve absolute smoothness. The polished specimen was rinsed with clean water, corroded by three potassium reagents, dried by the cold air of a blower, and placed in a self-sealing bag for testing.

2.2. Experimental methods

After the metallographic preparation of the specimen, the morphology and thickness of the cross-section of the specimen were observed and measured by a Keyence VHX-5000 super-depth-of-field microscope. The micromorphology of the specimen was analysed by a Hitachi S4800 scanning electron microscope and energy dispersive spectrometer, and a Bruker D8 Focus diffractometer (Germany) was used to analyse the phase composition of the specimens before and after friction and wear testing. The scanning angle ranged from 20° to 90°, and the scanning speed was 6°/min. The microhardness of the surface of the boronized layer was tested by an MH-6-type microhardness tester, and the hardness and microhardness of the boronized layer were observed by indentation.

The average friction coefficient curve is obtained by the wear tester HT-1000, the wear rate is calculated according to the mass change by using the delicate scale, and a Si_3N_4 ceramic ball with a diameter of 6 mm is used as a counterpart during the 45-minute wear test to study the tribological performance.

According to the VDI3198 [16] standard, the standard Daimler-Benz Rockwell-C test was used to evaluate the adhesion of the boronized layer, as shown in Fig. 1. The obvious deformation and fracture of the substrate metal and the boronized layer are caused by the applied load. The failure type of the boronized layer surface shows the cohesion of the layer. HF1-HF4 classifications indicate the adhesion strength of the boronized layer is sufficient while HF5 and HF6 classifications indicate the adhesion strength of boronized layer is insufficient.

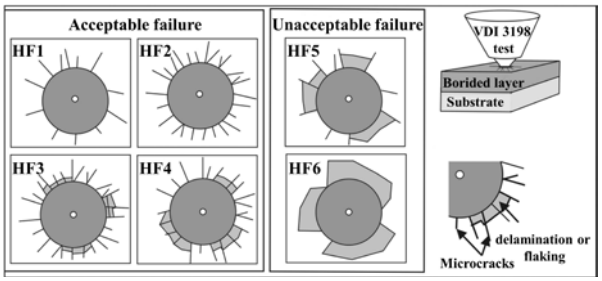

Fig. 1. Classification standards of the VDI 3198 test [16]

3. RESULTS AND DISCUSSION

3.1. Surface boronized layer thickness and analytical characterization

Fig. 2 shows the metallographic cross-section of the boronized layer boronized at 900 ℃ for 5 h. The boronized layer is tooth-shaped. Five locations were selected to measure the thickness of the boronized layer, as shown in Fig. 1, and the average value was taken [17]. Fig. 3 shows the average thickness of the boronized layer. The thickness of the boronized layer increases with increasing temperature and time. The thickness of the boronized layer is thinner at 800 ℃, approximately 35.6 μm ~ 70.90 μm. The thickness of the boronized layer at 900 ℃ increases significantly, reaching 107.34 μm. The thickness of the boronized layer at 1000 ℃ is almost 187.08 μm. The increase in the thickness of the boronized layer is significant in the first 5 hours, with

a maximum increase of approximately 64.45 μm, and the thickness increases slowly in the next 5 to 7 hours. The long boronizing time requires more energy consumption in the boronizing treatment process.

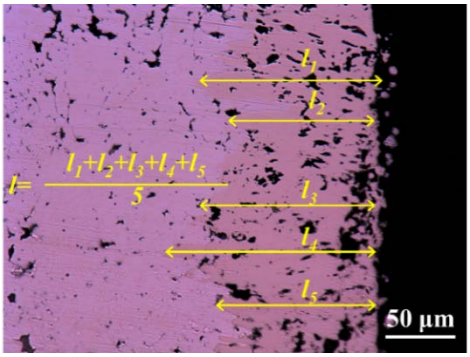

Fig. 2. Metallographic section of the specimen and method used to measure the thickness of the boronized layer

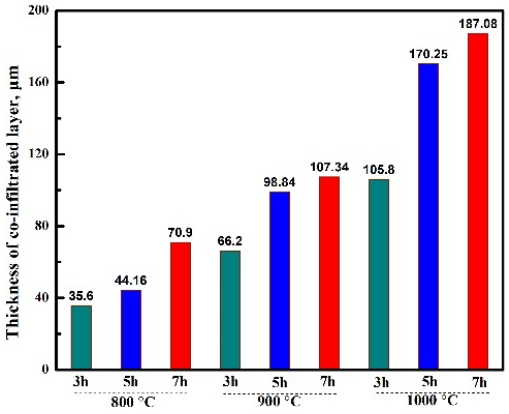

Fig. 3. Histogram of boronized layer thickness

The thickness of the boronized layer is proportional to the boriding temperature and the boriding time. Boriding is a diffusion reaction. The B atoms diffuse faster as the boriding temperature increases and more B atoms diffuse as the boriding time increases. Both above will cause the increase of thickness of the layer [18].

Fig. 4 shows the microstructure of the cross-section of the specimen after boronizing at 1000 ℃ for 5 h. The thickness of the boronized layer is approximately 170 μm. The shape is relatively flat, the tooth shape is not obvious, and irregularly shaped pores are obvious in the boronized layer, which are caused by the pores of the iron-based material itself and the pores left by atomic diffusion during the boronizing process. The surface layer of the specimen has a very thin FeB structure, which appears light blue after corrosion by a tripotassium reagent (1 g potassium ferrocyanide ($K_4Fe(CN)_6 \cdot 3H_2O$), 10 g potassium ferricyanide ($K_3Fe(CN)_6$), 30 g potassium hydroxide (KOH) codissolved in 100 mL water). The boronized layer is basically composed of Fe_2B.

Fig. 5 shows the microhardness curve of the specimen borided for 5 hours. The highest hardness value appears in the subsurface layer instead of the outermost layer because of the looseness of the surface layer [19]. Defects like decompaction, pores and cracks are brought to the outermost layer of the specimen at 1000 ℃. Dual-phase (the FeB phase with boron-rich and the Fe_2B phase with iron-rich) is located in the boronized layer of specimen at 1000 ℃. The boronized layer eventually results in increased brittleness and reduced adhesion to the substrate because there are major disparities in the thermochemical coefficient of expansion between the dual-phase. As a result, the highest hardness of the specimen at 1000 ℃ located in the subsurface layer, about 110 μm from the outermost layer. The microhardness of the remaining boronized layer (900 ~ 1500 $HV_{0.5}$ approximately) is much higher than that of the substrate which is 200 $HV_{0.5}$ approximately when the decompaction part is removed from the outermost layer.

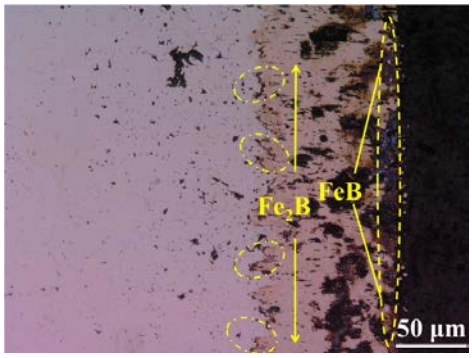

Fig. 4. Section of the specimen borided at 1000 ℃ for 5 h

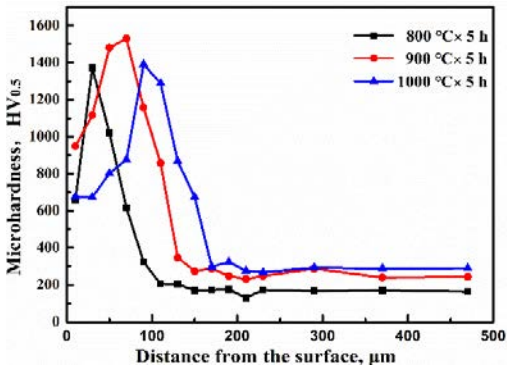

Fig. 5. Microhardness of specimens borided at different temperatures for 5 h

3.2. Daimler-Benz Rockwell-C adhesion test

The Daimler-Benz Rockwell-C adhesion test was used to evaluate adhesion between the boronized layer and the substrate after holding for 5 hours at different temperatures according to the HF1-HF6 indentation test (Fig. 1). SEM images of the indented specimens borided at 800 ℃, 900 ℃, and 1000 ℃ are shown in Fig. 6. There are only a few cracks in the specimen borided at 900 ℃ (Fig. 6 b), and the adhesive strength quality of the boronized layer classifies it as HF3.

The results indicate that the adhesive strength quality of the surface boronized layer is acceptable. However, in Fig. 6 a, the boronized layer treated at 800 ℃ delaminates or spalls around the perimeter of the indentation pits. In addition, the specimen borided at 1000 ℃ exhibits more delamination and spalling failures as well as visible ring cracks around the perimeter of the indentation pits than the specimen borided at 900 ℃ (Fig. 6 c). It is obvious that the binding between the boronized layer and the substrate borided at 900 ℃ is superior to that borided at 800 ℃ and 1000 ℃. The boronized layer is toothed and tightly embedded in the substrate at 900 ℃, and the boronized layer

consists of single-phase Fe_2B, which leads to a relatively compact structure. The ability of the boronized layer treated at 800 °C to resist extrusion stress is reduced due to the thin boronized layer. Spalling occurs easily when a certain load is applied, with delamination or spalling occurring around the perimeter of the indentation pits.

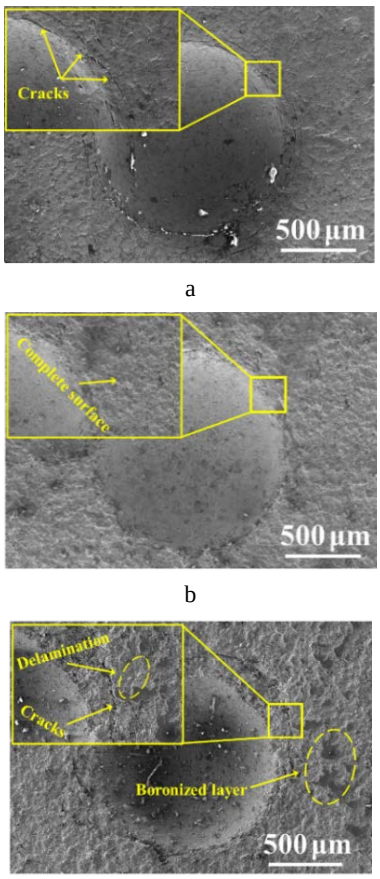

Fig. 6. Indentation marks on the surface of boride specimens treated at different temperatures for 5 h from the VDI adhesion test: a – 800 °C; b – 900 °C; c – 1000 °C

Due to the high temperature, more holes form in the boronized layer treated at 1000 °C, and the density decreases. The boronized layer becomes easy to peel off and break under external force at 1000 °C because of the major disparities in thermochemical coefficient of expansion between the dual-phase in the boronized layer of specimen at 1000°C causes increases the internal stress and brittleness of the boronized layer [20].

Therefore, the boronized layer has the best adhesion strength to the substrate at 900 °C [21].

3.3. Friction and wear behaviour

Fig. 7 shows the room-temperature coefficient of friction curves of the boride specimen treated at 800 °C, 900 °C and 1000 °C for 5 hours and with a load of 10 N and a sliding speed of 560 r/min for 45 min. The directly sintered specimen (unboronized specimens) was also tested for comparison. The specimen was sintered with a pressure of 3.5 MPa ~ 5.5 MPa at 1000 °C for 3 h. The friction coefficients of the boride specimens are higher than those of the unboronized specimens because iron-based materials prepared by powder metallurgy have more surface pores, a lower density, more crystal defects, and a nonuniform distribution, and it is easy to adsorb active boron atoms on surfaces at high temperature to form FeB or Fe_2B, resulting in the formation of new phases on the surface. The unreacted substances dope with each other to increase the peaks and valleys on a flat surface. Therefore, the surface roughness value increases, and the roughness of the unboronized specimen is lower than that of the specimens after boronizing. The oxidation resistance of the unboronized specimen is significantly lower than that of the boronized specimen. The temperature of the contact area between the surface of the specimen and the ceramic ball increases due to friction. The surface layer is oxidized eventually, the outermost layer in the air is equivalent to a "solid lubricant".

The oxide layer on the surface of the material acts as a "lubricant agent" now, which has certain friction reducing effect, so its friction coefficient is relatively low [22]. The wear diagram in Fig. 8 shows that the wear loss of the unboride specimen is significantly higher than that of the boronized specimens. These results indicate that a proper boronizing process can reduce mass loss and improve wear resistance.

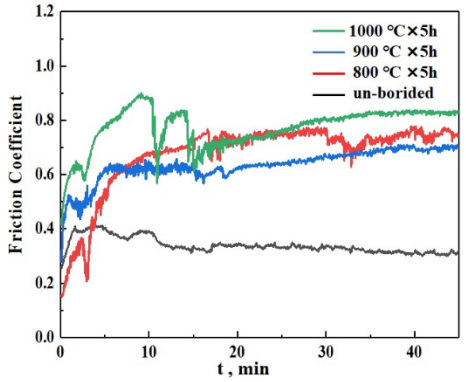

Fig. 7. Friction coefficient curve

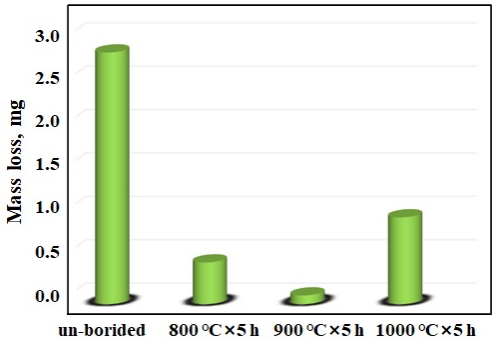

Fig. 8. Mass loss of different specimens

The specimen borided at 900 °C for 5 h has the lowest friction coefficient. The friction coefficient of the curve fluctuated slowly in the first 15 minutes, continued to rise to 0.6, and then remained relatively stable, and the friction coefficient increased relatively slowly. This shows that the boronized layer on the surface of the specimen has not lost its characteristics and suffers no obvious damage.

Fig. 9 shows the morphology of the worn surface at different temperatures. The friction coefficients of the specimens borided at 800 °C and 1000 °C for 5 h at room temperature are higher than those of the specimens borided at 900 °C, and the curve fluctuates sharply (Fig. 9 a, c).

Compared with the specimens boronized at 900 °C, the friction coefficients of the specimens boronized at 800 °C and 1000 °C for 5 hours are higher and the curve fluctuates severely (Fig. 9 a, c).

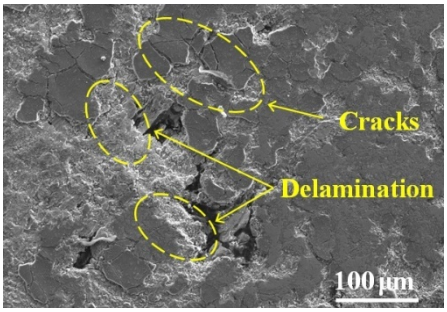

a

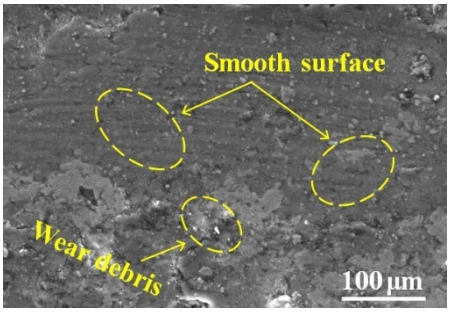

b

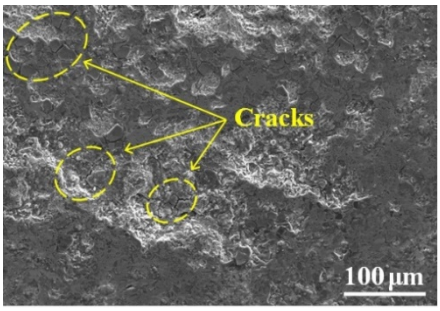

c

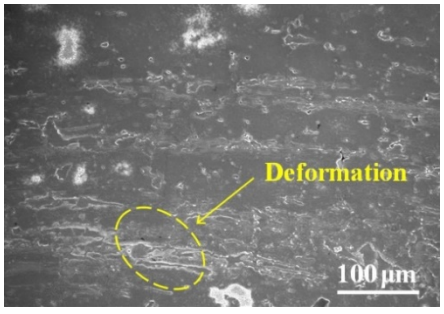

d

Fig. 9. Micromorphology of the wear specimens borided at different temperatures: a – 800 °C × 5 h; b – 900 °C × 5 h; c – 1000 °C × 5 h; d – unborided

Which is caused by micro cracks and plastic deformation, and both above are caused by the cyclic load stress in the wear test [23]. The surface of the unborided specimen will soften during friction and wear, and the hardness will decrease. When the load exceeds its bearing limit, the surface of the specimen is prone to fatigue, strong plastic deformation, and crack initiation. The appearance of cracks causes accelerated oxidation of the specimen surface. Many microcracks, obvious scratches and material tear appear on the worn surface of the unboride specimen after the wear test, as shown in Fig. 9 d.

Friction leads to an increase in the temperature of the contact zone, and the thermal stress caused by the thermal expansion mismatch between the boronized layer and the base material can lead to crack initiation. There was more exfoliation of the boronized layer in the specimens borided at 800 °C and 1000 °C than in the specimens borided at 900 °C, and the wear mechanism was different from that of the unboride specimens (Fig. 9 a, c). In both specimens, crack formation and propagation eventually led to a delamination wear mechanism. The temperature used to sinter the specimen borided at 800 °C is relatively low, resulting in insufficient sintering and a thinner layer, and the applied load causes the boronized layer to crack and fall off. In addition to a large amount of wear caused by the exfoliated borides, a portion of the exfoliated borides was crushed into hard particles at the wear surface, which transiently increased the friction factor, consistent with the large fluctuations in the friction factor curve of the specimen borided at 800 °C in Fig. 7. Many defects like decompaction, pores and cracks are brought to the borided layer of the specimen. at 1000 °C. The serrated tip at the end gradually passivates and the adhesion strength of the boronized layer decreases and the brittleness increases. It is squeezed and peeled off in the friction and wear test, resulting in a higher friction coefficient and wear amount (Fig. 8). The same situation was not observed on the specimen borided at 900 °C for 5 h, and the surface was relatively flat, with very few peeled areas. The SEM results of the above boride specimens are consistent with the Rockwell-C adhesion test conclusions.

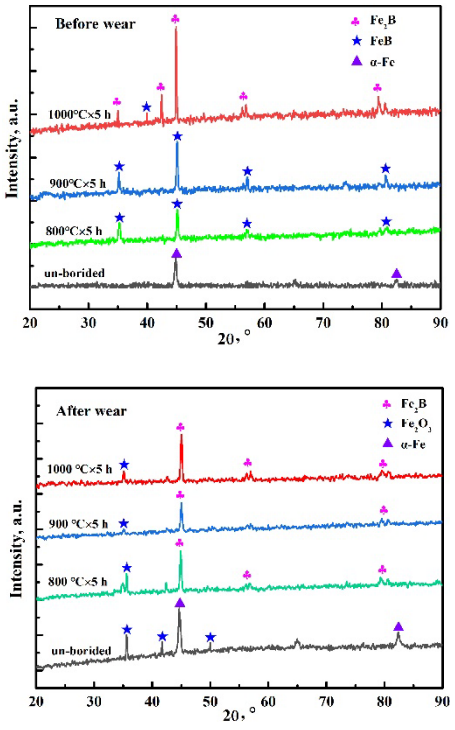

Fig. 10. XRD patterns of each specimen before and after the wear test

Fig. 10 shows the XRD phase analysis of the specimens before and after boronizing and before and after wear. The diffraction peaks of the specimens borided at 800 °C and 900 °C are attributed to single-phase Fe_2B. This is because when the temperature of the FeB phase increases, the B atoms have a strong diffusivity and easily and quickly diffuse into the metal, which makes it difficult to form the FeB phase in the boronized layer.

The unborided specimen surface mainly contains the α-Fe phase. After boronizing, the surface of the worn specimen is mainly composed of Fe_2B, Fe_2O_3 and α-Fe. The graph shows that Fe_2O_3 appears on the worn surface of the unborided specimen. The positions are greater than those after boronizing, indicating that the oxidation resistance of the specimens after boronizing is better than that of untreated specimens [24, 25].

To determine the wear mechanism, the cross-sectional structure and composition of the worn surface layer of the unboride specimen and the boride specimen (900 ℃ × 5 h) were compared and analysed. Fig. 11 a and b show the section wear morphology of the two cases, and it can be seen that there are obvious differences in the two morphologies.

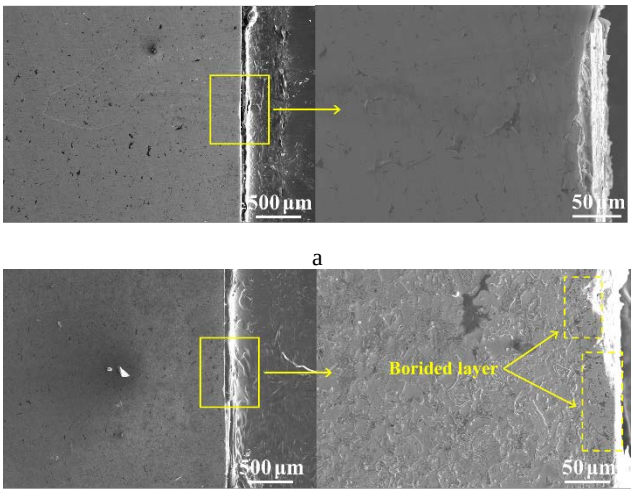

Fig. 11. Section of worn specimens: a – unborided; b – 900 ℃ × 5 h

The obvious plastic deformation with un-borided specimen is shown in Fig. 11 a, which indicates that the material softens and the yield strength decreases [26]. The grains on the surface are refined and begin to deform along the direction of friction, the surface layer is oxidized eventually after O atoms diffuse into the surface of the material, and then it acts as "solid lubricant" to reduce wear until it peels off. The formation and peeling of the oxide layer alternately proceed in the process of the wear test, which caused more mass loss and the friction curve is more stable and lower than that of the boride specimen.

There is no obvious plastic deformation with boride specimen near the surface oxide layer is shown in Fig. 11 b. The remaining boronized layer after wear test is still attached to the substrate. This is because the uniform and dense boronized layer that closely combined with the substrate supports this phenomenon [27].

4. CONCLUSIONS

1. The process parameters of boronizing treatment affect the thickness of the boronized layer absolutely. The better performance with reasonable thickness of boronized layer can be obtained by optimizing the process parameters. Defects like decompaction will be more obvious when the layer is too thin or too thick.
2. The dual-phase (Fe_2B, FeB) is generated at 1000 ℃, which leads to more holes on the surface of the specimen, and decreases of the adhesion to the substrate. The surface hardness of it is lower than that of the specimen with 900 ℃.
3. The boronized specimens obtain the best wear resistance and the lowest friction factor at 900 ℃ for 5 h. Delamination and oxidative wear caused by microcracks in the test are the main wear mechanisms of boronized specimens.

Acknowledgments

The authors gratefully acknowledge the support of the University Natural Science Foundation of Anhui (KJ2017ZD50), University support program for young talents of Anhui (gxyq2019186) and University Quality Project Foundation of Anhui (2019kfkc277).

REFERENCES

1. **Fujiki, A.** Present State and Future Prospects of Powder Metallurgy Parts for Automotive Applications *Materials Chemistry & Physics* 67 2001: pp. 298. https://doi.org/10.1016/S0254-0584(00)00455-7
2. **Lu, Y.H.** Study on the Preparation, Property and UItrasonic Fatigue Behavior of High-performance Iron-based Powder Metallurgy Sintered Material Guangdong: Doctoral Dissertation of South China University of Technology, 2014.
3. **Balusamy, T., Sankara Narayanan, T.S.N., Ravichandran, K.** Pack Boronizing of AISI H11 Tool Steel: Role of Surface Mechanical Attrition Treatment *Vacuum* 97 2013: pp. 36 – 43. https://doi.org/10.1016/j.vacuum.2013.04.006
4. **Wang, L., Wu, Y.M., Bian, G.Y.** Effect of Rare Earth La_2O_3 on Performance of 45 Steel Boronized Layer *Surface Technology s* 48(2) *s* 2019: pp. 94-99.
5. **Dybkov, V.I., Lengauer, W., Barmak, K.** Formation of Boronized Layers at the Fe-10%Cr Alloy-Boron Interface *Alloys Compound* 398 (1) 2005: pp. 113 – 122.
6. **Balusamy, T., Sankara Narayanan, T.S.N., Ravichandran, K.** Effect of Surface Mechanical Attrition Treatment (SMAT) on Pack Boronizing of AISI 304 Stainless Steel *Surface and Coatings Technology* 232 2013: pp. 60 – 67. https://doi.org/10.1016/j.surfcoat.2013.04.053
7. **Yuan, Q.L., Cao, J.J.** Effect of Boronization Technology on Microstructure and Properties of Boronizing Layer on 45 Steel *Hot Working Technology* 39 (2) 2010: pp. 134 – 136. https://doi.org/10.3969/j.issn.1001-3814.2010.02.044

8. **Ibrahim, G., Yusuf, K.** Investigation of Mechanical Properties of Borided Nickel 201 Alloy *Materials and Design* 53 2014: pp. 577 – 580. https://doi.org/10.1016/j.matdes.2013.07.001
9. **Vipin, J., Sundararajan, G.** Influence of the Pack Thickness of the Boronizing Mixture on The Boriding of Steel *Surface and Coatings Technology* 149 (1) 2002: pp. 21 – 26. https://doi.org/10.1016/S0257-8972(01)01385-8
10. **Xie, F., Sun, L. Cheng, J.** Alternating Current Field Assisted Pack Boriding to Fe_2B Coating *Surface Engineering* 29 (3) 2013: pp. 240 – 243. https://doi.org/10.1179/1743294412Y.0000000104
11. **Keddam, M., Chentouf, S.M.** A Diffusion Model for Describing the Bilayer Growth (FeB/Fe_2B) During the Iron Powder-Pack Boriding *Applied Surface Science* 252 (2) 2005: pp. 393 – 399. https://doi.org/10.1016/j.apsusc.2005.01.016
12. **Uslu, I., Comert, H., Ipek, M.** Evaluation of Borides Formed on AISI P20 Steel *Material & Design* 28 (1) 2007: pp. 55 – 61. https://doi.org/10.1016/j.matdes.2005.06.013
13. **Gómez-Vargas, O.A., Keddam, M., Ortiz-Domínguez, M.** Kinetics and Tribological Characterization of Pack-Borided AISI 1025 Steel *High Temperature Materials and Processes* 36 (3) 2016: pp. 197 – 208. https://doi.org/10.1515/htmp-2015-0199
14. **Telasang, G., Dutta Majumdar, J., Padmanabham, G.** Wear and Corrosion Behavior of Laser Surface Engineered AISI H13 Hot Working Tool Steel *Surface & Coatings Technology* 261 (15) 2015: pp. 69 – 78. https://doi.org/10.1016/j.surfcoat.2014.11.058
15. **Ramdane, N., Touhami, M.Z., Khettache, A.** Boriding and Boronitrocarburising Effects on Hardness, Wear and Corrosion Behavior of AISI 4130 Steel *Revista Matéria* 24 (1) 2019: pp. 12316 – 12327. https://doi.org/10.1590/S1517-707620190001.0609
16. **Vidakis, N., Antoniadis, A., Bilalis, N.** The VDI 3198 Indentation Test Evaluation of a Reliable Qualitative Control for Layered Compounds *Journal of Materials Processing Technology* 143 – 144 2003: pp. 481 – 485. https://doi.org/10.1016/S0924-0136(03)00300-5
17. **Huang, X., Cui, M.X., Lai, D.O.** Study on Solid-Boronizing Process with Rare Earth Elements Catalysis for 45 Steel *Hot Working Technology* 42 (10) 2013: pp. 194 – 197.
18. **Fang, H.M., Zhang, G.S., Xia, L.S.** Properties of Sintering-Boronized for Fe-based Powder Metallurgy Material *Key Engineering Materials* 866 2020: pp. 104 – 110. https://doi.org/10.4028/www.scientific.net/KEM.866.104
19. **Ptačinová, J., Drienovský, M., Palcut, M.** Oxidation Stability of Boride Coatings *Kovove Materialy* 53 (3) 2015: pp. 175 – 186. https://doi.org/10.4149/km_2015_3_175
20. **Mustafa, S.G., Yılmaz, K., Azmi, E.** Dry Sliding Wear Behavior of Borided Hot-Work Tool Steel at Elevated Temperatures *Surface & Coatings Technology* 328 2017: pp. 54 – 62. https://doi.org/10.1016/j.surfcoat.2017.08.008
21. **Yusuf, K., Ylmaz, Y., Sukru, T.** Adhesion and Wear Properties of Boro-tempered Ductile Iron *Material & Design* 32 (8 – 9) 2011: pp. 4295 – 4303. https://doi.org/10.1016/j.matdes.2011.04.014
22. **Azmi, E.** Investigation of High Temperature Dry Sliding Behavior of Borided H13 Hot Work Tool Steel with Nanoboron Powder *Surface & Coatings Technology* 357 2019: pp 886 – 895. https://doi.org/10.1016/j.surfcoat.2018.10.066
23. **Fang, H.M., Xu, F.** Research on Properties of Fe-based Powder Metallurgy Material Strengthened by Boriding *Strength of Materials* 52 (4) 2020: pp. 621 – 626. https://doi.org/10.1007/s11223-020-00214-6
24. **Kaya, H.** Solid Particle Erosion Wear Behavior of Severe Plastically Deformed AA7075 Alloys *Materials Testing* 60 2018: pp. 885 – 891. https://doi.org/10.3139/120.111227
25. **Esgin, U., Özyűrek, D., Kaya, H.** Investigation of Wear Behavior of Precipitation-Strengthened Nickel-Copper Based K-500 Alloy Produced by Powder Metallurgy *Acta Physica Polonica A* 129 2016: pp. 544 – 547. https://doi.org/10.12693/APhysPolA.129.544
26. **Wibberley, R., Eyre, T.S.** The Dry Sliding Wear Characteristics of Copper with and without 0.08% Silver *Wear* 13 (1) 1969: pp. 27 – 38. https://doi.org/10.1016/0043-1648(69)90429-3
27. **Mykhaylo, P., Krzysztof, D., Jerzy, J.** Analysis of Wear Resistance of Borided Steel C45 *Materials (Basel)* 13 (23) 2020: pp. 5529. https://doi.org/10.3390/ma13235529

© Fang et al. *2022* Open Access This article is distributed under the terms of the Creative Commons Attribution 4.0 International License (http://creativecommons.org/licenses/by/4.0/), which permits unrestricted use, distribution, and reproduction in any medium, provided you give appropriate credit to the original author(s) and the source, provide a link to the Creative Commons license, and indicate if changes were made.